

MOI-Mixer: Improving MLP-Mixer with Multi Order Interactions in Sequential Recommendation

Hoon Lee
hoonleesky@kaist.ac.kr
KAIST AI

Dongyoon Hwang
godnpeter@kaist.ac.kr
KAIST AI

Sunghwan Hong
sung_hwan@korea.ac.kr
Korea University

Changyeon Kim
matthew.g@kakaocorp.com
KAKAO

Seungryong Kim
seungryong_kim@korea.ac.kr
Korea University

Jaegul Choo
jchoo@kaist.ac.kr
KAIST AI

ABSTRACT

Successful sequential recommendation systems rely on accurately capturing the user’s short-term and long-term interest. Although Transformer-based models achieved state-of-the-art performance in the sequential recommendation task, they generally require *quadratic* memory and time complexity to the sequence length, making it difficult to extract the long-term interest of users. On the other hand, Multi Layer Perceptrons (MLP)-based models, renowned for their *linear* memory and time complexity, have recently shown competitive results compared to Transformer in various tasks. Given the availability of a massive amount of the user’s behavior history, the linear memory and time complexity of MLP-based models make them a promising alternative to explore in the sequential recommendation task. To this end, we adopted MLP-based models in sequential recommendation but consistently observed that MLP-based methods obtain lower performance than those of Transformer despite their computational benefits. From experiments, we observed that introducing explicit high-order interactions to MLP layers mitigates such performance gap. In response, we propose the Multi-Order Interaction (MOI) layer, which is capable of expressing an arbitrary order of interactions within the inputs while maintaining the memory and time complexity of the MLP layer. By replacing the MLP layer with the MOI layer, our model was able to achieve comparable performance with Transformer-based models while retaining the MLP-based models’ computational benefits.

CCS CONCEPTS

• Information systems → Recommender systems.

KEYWORDS

Sequential Recommendation; MLP; PARAFAC

1 INTRODUCTION

A sequential recommendation system is a core component for personalized recommendation services in Internet service platforms such as e-commerce, social network, and Over-the-top media. Given a sequence of a user’s historical behaviors, the prediction performance of a sequential recommendation system depends on accurately capturing the user’s short- and long-term interest, referred as temporal dynamics. To this end, early work utilized Markov Chains [27] or Recurrent Neural Networks (RNN) [11] to represent the temporal dynamics within the user’s historical behaviors.

Over the past decades, Internet service platforms accumulated a massive amount of user behavior history with extremely long lengths [26, 37]. With the availability of such data, extracting users’ long-term interest has become a key challenge for constructing an effective sequential recommendation system. However, RNN-based architectures struggle to propagate information through long sequences due to the vanishing gradient problem [12]. As an alternative, Transformer [35] was proposed to overcome the limitations of RNNs by using a self-attention layer. The self-attention layer constructs input-dependent attention weights which provide a global receptive field over the entire sequence and directly connect all the items (e.g., tokens) in the sequence. With such a global receptive field, Transformer effectively extracts the user’s long-term interest and attains state-of-the-art performance in natural language processing [4] and sequential recommendation tasks [16, 29].

Although the self-attention layer successfully extracts users’ long-term interest, the attention weights make the memory and time complexity *quadratic* to the sequence length and this restricts the applicability of Transformer-based models from processing extremely long sequence data. Recently, MLP-based architectures [22, 31, 33, 38], including MLP-Mixer [32], have been proposed to replace the self-attention layer in Transformer with a simple MLP layer. The MLP layer integrates the items in the sequence with linear layers, successfully reducing the quadratic complexity to a linear complexity by substituting the self-attention layer. Surprisingly, these architectures achieved competitive performance in comparison to Transformer for natural language processing. With the availability of the users’ long behavior history, the linear computational cost of the MLP layers is indeed an attractive and promising direction to explore in the sequential recommendation systems.

From our extensive experiments, we observed that MLP-based methods performed relatively worse than Transformer-based methods for the sequential recommendation task despite its computational benefits. One of the convincing reasons could be the difference in the order of interactions a MLP layer and a self-attention layer exploit. The MLP layer contains a first-order interaction term (e.g., Wx) whereas a self-attention layer contains a third-order interaction term (e.g., $qk^T v$). Although the first-order interaction term of the MLP layer is a universal function [13], several architectures that explicitly utilize complex interaction terms [14, 15, 24] have shown their effectiveness for the sequential recommendation task. Therefore, in this paper, we study the potentials of high-order interaction terms in the sequential recommendation task.

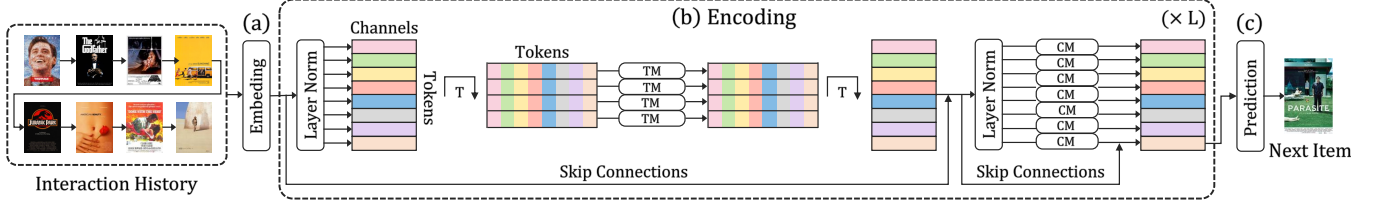


Figure 1: The overall architecture of MOI-Mixer which consists of 3 different modules: (a) an embedding; (b) an encoding; and (c) a prediction module. The goal is to predict the next interacted item based on the user’s interaction history.

We propose a novel Multi-Order Interaction (MOI) layer designed to capture the desired k -th order interactions, while maintaining the linear computational cost of the MLP layer. By replacing MLP layers in MLP-Mixer with our MOI layers, we named our model as MOI-Mixer. Note that MLP-Mixer is a special case of MOI-Mixer since the MOI layer with interaction order at $k = 1$ is identical to the MLP layer. MOI-Mixer alternates between (i) a token-mixing layer, which integrates the representations across tokens, and (ii) a channel-mixing layer, which integrates the representations within each token. We conducted extensive experiments on various datasets and observed that high-order interactions for the channel-mixing operation improves the performance of MOI-Mixer.

In summary, our contributions are threefold as follows:

- To the best of our knowledge, we are the first to apply various state-of-the-art MLP-based architectures in sequential recommendation systems.
- We propose a novel Multi-Order Interaction (MOI) layer, which effectively expresses the arbitrary order of interaction within the inputs and stacked them to construct MOI-Mixer.
- Through extensive experiments, we observe that MOI-Mixer surpasses existing MLP-based architectures, which validates the effectiveness of the high-order interactions in the sequential recommendation tasks.

2 RELATED WORK

2.1 Sequential Recommendation

Sequential recommendation systems are based on the user’s previous sequential behaviors to anticipate their future behavior. To address this problem, early work such as FPMC [27] attempts to learn user-specific transition matrices using Markov chains to model sequential patterns. Inspired by neural models’ strong representation capabilities, deep learning-based approaches [10, 11, 30, 36] including recurrent and convolution neural networks have been proposed to learn complicated user behaviors and effectively capture long-term dependencies. Recently, Transformer [35] directly connects all the items in the sequences and successfully extracts the user’s long-term preferences. These methods achieved state-of-the-art performance in sequential recommendation [16, 29].

2.2 MLP-based Architectures

Transformer architecture with the self-attention layer has attained state-of-the-art performance in various tasks including computer

vision [3, 6] and natural language processing [4]. However, recent studies have shown that MLP-based architectures [22, 31–33, 38] can achieve competitive performance against Transformer for both computer vision and natural language processing. These MLP-based models have similar macro-level architecture to Transformer but differ in the micro-component designs. MLP-Mixer [32] and ResMLP [33] simply replaced the self-attention layer with the MLP layer and obtained competitive performance on image classification benchmarks. gMLP [22] used the gated version of the MLP layer, further enhancing the performance of the MLP-based models.

3 PRELIMINARY

This section describes the problem settings of sequential recommendation and the macro-level architecture of MOI-Mixer.

3.1 Problem Formulation

Sequential recommendation aims to model the users’ item preference by predicting the next item given the past interacted items (i.e., watched movies) [16, 29]. Formally, given a sequence of users’ interacted items with length s , at time step t (i.e., interacted items from time step $t - s + 1$ to t), the objective is to predict the next item at time step $t + 1$ that the user is likely to interact with.

3.2 Overall Architecture

Fig. 1 depicts the overall architecture of MOI-Mixer. MOI-Mixer closely follows the macro-structure of MLP-Mixer and ResMLP [32, 33], which is composed of three different modules: (a) an embedding, (b) an encoding, and (c) a prediction module.

The embedding module in Fig. 1(a) takes a sequence of s number of items in the user’s item interaction history as an input, and each item is projected onto a c -dimensional token resulting in an input matrix of $X \in \mathbb{R}^{s \times c}$. Note that while previous architectures with self-attention layers utilized positional embedding to provide either absolute or relative positional information in a given sequence to cope with the permutation invariance property [16, 29], MOI-Mixer does not require the positional embedding since the encoding layer within our proposed architecture is already sensitive to the order of the tokens, allowing inherent learning of position of each sequence.

Then, in Fig. 1(b), the embedded input X is fed into the encoder module which consists of a stack of identical blocks where each block is composed of two mixing operations. The first operation conducts token-wise mixing, which we call a token-mixing layer, $TM(\cdot)$. It acts identically on the columns of X to capture the interaction between the tokens within a channel which maps $\mathbb{R}^s \mapsto \mathbb{R}^s$. Then,

the results are fed to a channel-mixing sub-layer, $CM(\cdot)$, which acts on the rows of X to capture the interaction between the channels within a token, which maps $\mathbb{R}^c \mapsto \mathbb{R}^c$. Following [29, 32, 33], standard architectural components such as residual connections [7] and layer normalization [2] are utilized to stabilize the training process. Omitting the layer indices for brevity, the encoder layer of MOI-Mixer is written as

$$\begin{aligned} Y_{*,i} &= X_{*,i} + TM(\text{LayerNorm}(X)_{*,i}), \quad \text{for } i = 1 \dots c, \\ Z_{j,*} &= Y_{j,*} + CM(\text{LayerNorm}(Y)_{j,*}), \quad \text{for } j = 1 \dots s, \end{aligned} \quad (1)$$

where $Y, Z \in \mathbb{R}^{s \times c}$ indicates the output of the token-mixing layer and the channel-mixing layer, respectively.

Once the input undergoes the encoding module, the encoded representation of the last token $X_s \in \mathbb{R}^c$ in the sequence is passed to the prediction module for the final classification problem, as shown in Fig. 1(c). The prediction module is composed of a two-layer feed-forward network with GELU activation [9], followed by the softmax function as done in [29]. As a result, we obtain a probability distribution over the items for the next token.

The difference between the MLP-Mixer [32] and ours lies on the operations of the token-mixer $TM(\cdot)$ and the channel-mixer $CM(\cdot)$. The MLP-Mixer utilized a MLP layer for $TM(\cdot)$ and $CM(\cdot)$, capturing the first-order interactions between the tokens and the channels. However, MOI-Mixer applies the MOI layer, capturing the multi-order interactions between the tokens and the channels.

4 PROPOSED METHOD

Here, we explain our MOI (Multi-Order Interaction) layer designed to capture the multi-order interaction over the input features.

4.1 Parameterized Multi-Order Interaction

Our goal is to learn a weight tensor \mathcal{T} which linearly combines the k -th order of interaction between k different inputs. Let us denote the input vectors as $x_1 \in \mathbb{R}^{d_1}, \dots, x_k \in \mathbb{R}^{d_k}$, the number of the hidden dimensions as d_1, \dots, d_k , the desired order of interaction as k and the output dimension as h . In addition, we define the learnable tensor $\mathcal{T} \in \mathbb{R}^{d_1 \times \dots \times d_k \times h}$, which outputs h different k -th order interactions over the input features denoted by $z \in \mathbb{R}^h$. Specifically, z is defined as

$$z^T = (((\mathcal{T} \times_1 x_1) \times_2 x_2) \times_3 \dots \times_k x_k), \quad (2)$$

where operator \times_i denotes the i -th mode tensor product.

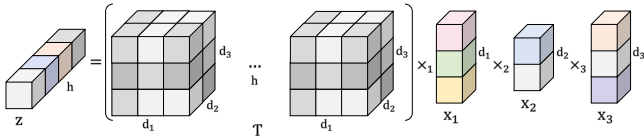


Figure 2: An illustrative example of the Parameterized Multi-Order Interaction for the interaction order $k = 3$.

4.2 Low-Rank Approximation

Although the tensor \mathcal{T} could capture all possible k -th order interactions, learning such a large tensor \mathcal{T} gets practically infeasible due

to the exponential number of parameters as mode k increases. To reduce the computational cost, we employ PARAFAC decomposition [17] to perform a low-rank approximation of the tensor. Note that we denote R as the rank of the decomposed matrices which controls a trade-off relationship between the decomposition rate and the computational cost. Here, we set as $R = 1$ and conduct the PARAFAC decomposition for the tensor \mathcal{T} , i.e.,

$$\mathcal{T} \approx (((\mathcal{G} \times_1 W_1) \times_2 W_2) \times_3 \dots \times_k W_k), \quad (3)$$

where $\mathcal{G} \in \mathbb{R}^{\overbrace{h \times h \times \dots \times h}^{k+1}}$ is a rank-1 weighting tensor and $W_1 \in \mathbb{R}^{d_1 \times h}, \dots, W_k \in \mathbb{R}^{d_k \times h}$ are the learnable factor matrices [5].

Then, leveraging Eq. (3), we can re-write the output z as

$$z^T \approx (((\mathcal{G} \times_1 x_1 W_1) \times_2 x_2 W_2) \times_3 \dots \times_k x_k W_k). \quad (4)$$

Following [21], the result obtained from Eq. (4) can be approximated by the Hadamard products without the presence of the rank-1 tensor \mathcal{G} . Hence the output z can be approximated as

$$z \approx (W_1^T x_1 \odot \dots \odot W_k^T x_k), \quad (5)$$

where \odot indicates the Hadamard product.

In Eq. (5), the weight matrices W_1, \dots, W_k can have their own bias vectors $b_1, \dots, b_k \in \mathbb{R}^h$. With the bias vectors, the output z can represent all terms of the interactions less than or equal to k , i.e.,

$$\begin{aligned} z &\approx (W_1^T x_1 + b_1) \odot \dots \odot (W_k^T x_k + b_k) \\ &= (\mathbf{Wx} + \sum_{i=1}^{i=k} \mathbf{Wx} \odot W_i^T x_i \cdot \text{diag}(b_i) \\ &\quad + \sum_{i=1}^{i=k} \sum_{j=i+1}^{j=k} \mathbf{Wx} \odot (W_i^T x_i \odot W_j^T x_j) \cdot \text{diag}(b_i \odot b_j) \\ &\quad + \dots + (b_1 \odot \dots \odot b_k)), \end{aligned} \quad (6)$$

where $\mathbf{Wx} = (W_1^T x_1 \odot \dots \odot W_k^T x_k)$ and \odot indicates the Hadamard division.

4.3 Multi-Order Interaction Layer

The interaction model in Eq. (5) outputs h different features of the k -th order interactions. We then introduce an additional linear layer $W_o \in \mathbb{R}^{h \times d}$ after the Hadamard product to not only aggregate, but also map the output z onto the identical dimension as input x for residual connections.

To further enhance the representative capacity of the model, we apply a non-linear activation function immediately after the input vectors, as in [19]. However, the Hadamard product over the multiple inputs may induce the explosion of the output values. Therefore, to suppress the large output values, we exploit an additional layer normalization after the product, inspired by [1, 39].

To sum up, as illustrated in Fig. 3, we define our MOI (Multi-Order Interaction) Layer at the interaction order k as

$$MOI_k(x_1, \dots, x_k) = W_o^T (\text{LayerNorm}(\sigma(W_1^T x_1) \odot \dots \odot \sigma(W_k^T x_k))), \quad (7)$$

where σ is an element-wise non-linear function (i.e., GELU [9]).

4.4 Special cases of MOI layer

We now discuss the relationship between the MOI layer and existing layers with respect to the order k . Throughout the section, we omit the normalization layer for brevity.

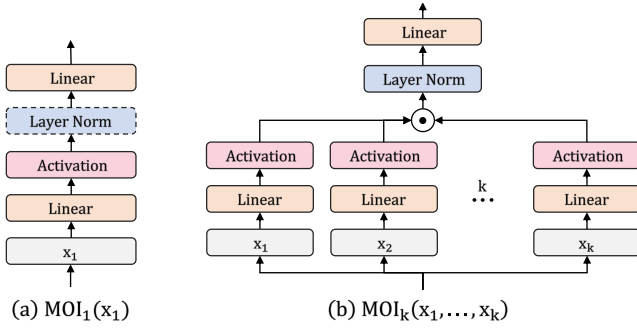


Figure 3: Our proposed MOI layer that captures the multi-order interaction between the input features.

MLP Layer For the case where the MOI layer’s order k is set to 1, it is identical to the MLP layer as shown in Fig. 3(a), i.e.,

$$MOI_1(x) = W_o^T (\sigma(W_1^T x)), \quad (8)$$

where $x \in \mathbb{R}^c$ denotes the input vector, $W_1 \in \mathbb{R}^{c \times h}$ and $W_o \in \mathbb{R}^{h \times c}$ denote the fully connected layers with a hidden dimension h , and σ is the activation function. Note that we do not need the normalization layer due to the absence of the Hadamard product.

Bilinear Pooling Layer For the case where the order of MOI layer is $k = 2$, the MOI layer is identical to the low-rank bilinear pooling layer proposed in [18, 19] which is defined as

$$MOI_1(x, y) = W_o^T (\sigma(W_1^T x) \odot \sigma(W_2^T y)), \quad (9)$$

where $x, y \in \mathbb{R}^c$ are input vectors, $W_1, W_2 \in \mathbb{R}^{c \times h}$ are weight matrices, σ is the activation and $W_o \in \mathbb{R}^{h \times c}$ is a pooling matrix.

4.5 MOI-Mixer

The final architecture of our proposed MOI-Mixer $_{(k_s, k_c)}$ is composed of two MOI layers, one for the token-mixing $TM(\cdot)$ layer, where k_s indicates the order of token interaction and one for the channel-mixing $CM(\cdot)$ layer, where k_c indicates the order of channel interaction. Since our goal is to introduce an explicit high-order term of the given input, we set all inputs x_1, \dots, x_k as a single input x in the MOI layer. We further denote the hidden dimension of $TM(\cdot)$ and $CM(\cdot)$, respectively, with d_s and d_c .

4.6 Relation to Previous Models

In this section, we give a detailed comparison between MOI-Mixer and relevant prior models [22, 32, 33].

Relation to MLP-Mixer, ResMLP : The overall structure of MOI-Mixer can easily be modified to MLP-Mixer [32] and ResMLP [33], the simplest MLP-based architecture, by simply setting the order of the MOI-Mixer $_{(k_s, k_c)}$ as $k_s = 1$ and $k_c = 1$ for the token-mixing $TM(\cdot)$ and the channel-mixing $CM(\cdot)$ layer. Note that ResMLP [33] requires an additional affine layer before and after the token-mixing layer for normalization.

Relation to gMLP : Different from the MLP-Mixer architecture,

gMLP combines the token-mixing and the channel-mixing in a single module which can be written as:

$$Z = (\sigma(XW_1) \odot W_s \sigma(XW_2))W_o, \quad (10)$$

where $X \in \mathbb{R}^{s \times c}$ is the input matrix, $W_1, W_2 \in \mathbb{R}^{c \times h}$ are channel-mixing weights, $W_s \in \mathbb{R}^{s \times s}$ is a token-mixing weight, and $W_o \in \mathbb{R}^{h \times c}$ is the output matrix.

By removing the token-mixing weight W_s , gMLP is identical to the channel-mixing layer $CM(\cdot)$ of MOI-Mixer with the order $k_c = 2$. Since the token’s interaction is modeled by a simple linear layer W_s , gMLP resembles MOI-Mixer when the interaction order of the token-mixer is $k_s = 1$ and channel-mixer is $k_c = 2$. However, MOI-Mixer differs from the gMLP where the gMLP’s computational costs of W_s is quadratic to the sequence length which may not be a practical choice for the long sequence dataset.

5 EXPERIMENTS

In this section, we first provide our experimental settings and report the results with detailed analysis on standard benchmark datasets. Specifically, Section 5.1 briefly introduces the datasets and evaluation protocols. Section 5.2 analyzes the effects of the interaction order. Then, Section 5.3 compares MOI-Mixer and its variants with state-of-the-art recommendation architectures to verify the effectiveness of high-order interactions. Lastly, Section 5.4 conducts an ablation study for an in-depth analysis of the proposed method.

5.1 Experimental Setup

Datasets We evaluate our model on five sequential recommendation datasets where the sparsity and domain varies significantly.

- *Beauty*: This is a dataset introduced in [25], containing series of product reviews crawled from the *Amazon.com*. This dataset is known for its high sparsity.
- *Steam*: This is a dataset collected from the online game distribution platform, *Steam*, which was first introduced in [16].
- *MovieLens*: This is a widely-used benchmark dataset in recommendation systems containing each user’s ratings for movies. We used MovieLens-1m and MovieLens-20m, where 1m and 20m indicate the number of interactions, respectively.
- *XLong*: This is a dataset introduced by [26], which is the collection of the click logs of Alibaba’s e-commerce platform, containing particularly long sequences of data.

Table 1: Statistics of the processed dataset. The avg. int. denotes the average number of interacted items per user.

| Type | Dataset | Users | Items | Total int. (M) | Avg. int. |
|-------|---------|---------|---------|----------------|-----------|
| Small | Beauty | 40,226 | 54,542 | 0.4 | 8.8 |
| | Steam | 281,428 | 13,044 | 3.5 | 12.4 |
| | ML-1m | 6040 | 3,416 | 1.0 | 163.5 |
| Large | ML-20m | 138,493 | 26,774 | 20.0 | 144.4 |
| Long | XLong | 20,000 | 747,460 | 15.9 | 794.2 |

We followed the data pre-processing procedure from [16, 29], where all reviews and ratings are regarded as implicit feedback.

Afterward, interacted items are grouped by users and ordered by timestamps. We only kept users and items that have at least five interactions to maintain the quality of the dataset. Detailed statistics of the processed datasets are outlined in Table 1.

Baselines To verify the effectiveness of our model, we compare our method with well-known sequential recommendation baselines including POP, NCF [8], GRU4Rec⁺ [11], HPMN [26] and BERT4Rec [29]. POP is one of the simplest baselines which recommends items based on rank-based popularity. NCF models the interactions between users and items via matrix factorization. While factorization-based methods [8] disregard the temporal dynamics of interaction histories, GRU4Rec⁺ utilize RNNs to incorporate the temporal dynamics. However, for datasets with longer sequences, the recurrent neural layers suffer from the vanishing gradient problem. To alleviate this problem, HPMN introduced a hierarchical memory network to the recurrent layers to memorize the user’s long-term interest. On the other hand, BERT4Rec utilized the self-attention layer to globally attend all items within the sequence. Apart from the sequential recommendation literature, we consider MLP-based architectures (i.e., MLP-Mixer [32] and gMLP [22]), which integrate the temporal dynamics with a simple MLP layer.

For POP and NCF we report the results from [29]. For GRU4Rec⁺ and HPMN we use the official code while modifying the prediction module identical to our settings. For BERT4Rec, MLP-Mixer, and gMLP, the results are based on our reproduced implementations.

Training For the training procedure, we adopted the masked language modeling (MLM), a conventional training objective for bidirectional sequential models [4, 29]. Specifically, we randomly masked tokens within the given sequence of historical behavior of a user and trained the model to predict the original item of the masked token based on its context.

Implementation Details For fair comparison, we set GRU4Rec⁺ and HPMN by following their optimal configurations where the number of layers are fixed as $L = 6$. For BERT4Rec, MLP-Mixer, gMLP, and MOI-Mixer, we use the optimal configurations of BERT4Rec. We trained all models by changing the learning rate from $\{1e - 3, 5e - 4, 3e - 4, 1e - 4\}$, weight decay from $\{1e - 3, 1e - 4, 1e - 5\}$ and report the best results averaged over three random seeds. Unless specified, we conducted experiments under the same experimental settings for all models and datasets, as follows:

- *Architecture*: We set the number of layers $L = 2$ and input hidden dimension $d_h = 256$. We closely follow the implementation details in [32] and set the hidden dimension d_s of token-mixer as half the input hidden dimension d_h , i.e., $d_s = \frac{1}{2}d_h = 128$. For the hidden dimension d_c of channel-mixer, we scale the dimension for each model to minimize the difference of the total number of parameters between models. We use $d_c = 3d_h = 768$ for BERT4Rec, $d_c = 4d_h = 1024$ for gMLP, and $d_c = \frac{6}{k_c+1}d_h$ for MOI-Mixer. When $k_c = 1$, the channel-mixing layer of MOI-Mixer is identical to the point-wise feed forward network of BERT4Rec.

Following [29], we initialized all parameters with a truncated normal distribution ranging from $[-0.02, 0.02]$ only except

for those of gMLP’s spatial gating unit. For the spatial gating unit, the weights are initialized nearly to zero and biases to one, in order to ensure the training stability as in [22].

- *Optimizer*: We used Adam [20] optimizer and trained for 200 epochs with cosine learning rate decay [23]. We set the batch size as 256 and dropout rate as 0.2.
- *Sequence Length*: Following [16, 29], we set the maximum sequence length as $s = 50$ for Beauty and Steam, and $s = 200$ for ML-1m and ML-20m datasets. For XLong dataset, we set s as 1000, following from [26]. The mask proportion ρ is fixed to $\rho = 0.6$ for Beauty, $\rho = 0.4$ for Steam, $\rho = 0.2$ for ML-1m, ML-20m, and $\rho = 0.1$ for XLong dataset.

Evaluation For evaluation, we adopted the next item recommendation (i.e., leave-one-out evaluation) task. For each user, we set the last item of the interaction sequence as the test data and the second-last item as the validation data. Here, the goal is to rank the ground-truth item higher than the other items. For fair comparison, we pair the ground-truth item with 100 negative items that are sampled according to their popularity following [8, 16, 28, 29].

Metrics When comparing among models, we are interested in two primary quantities: (1) the recommendation accuracy and (2) computational cost, which are major concerns of a recommendation system. To measure the recommendation accuracy, we commonly employ TOP-N metrics, *Hit Ratio* (HR) and *Normalized Discounted Cumulative Gain* (NDCG). Throughout this section, we compare HR@ n and NDCG@ n with rank n set to $\{1, 10\}$. To indicate the computational cost, we denote the number of parameters for the encoding layer (Params), the GPU memory requirements (VRAM) and the Floating point Operations Per Second (FLOPs).

5.2 Impact of Interaction Orders

Here, we empirically study the importance of the interaction order for the token- and channel-mixing layer. Throughout this section, we use ML-1m dataset for the evaluation.

Table 2: Effects of the token interaction orders on ML-1m.

| Model | k_s | k_c | Params (M) | NDCG@10 |
|-----------|-------|-------|------------|---------------|
| MOI-Mixer | 1 | 1 | 0.89 | <u>0.4805</u> |
| | 2 | 1 | 0.89 | 0.4782 |
| | 3 | 1 | 0.89 | 0.4674 |
| BERT4Rec | - | - | 1.31 | 0.4964 |

Order of token interaction Table 2 shows the comparison of MOI-Mixer to other methods with respect to various token interaction orders ranging from $k_s \in \{1, 2, 3\}$. Comparing the results among MOI-Mixer variants, MOI-Mixer_(1,1) (i.e., MLP-Mixer) shows the most competitive performance compared to BERT4Rec, with a 1.6% drop in NDCG@10. We observe that a simple first-order token interaction performs the best, while more complex token-wise interactions degrade the recommendation accuracy of MOI-Mixer.

Table 3: Performance of different recommendation models on next-item prediction. The results are averaged over three random seeds. Bold scores indicate the best model for each metric and underlined scores indicate the second best model.

| Datasets | Metric | POP | NCF | GRU4Rec ⁺ | HPMN | BERT4Rec | gMLP | MLP-Mixer | MOI-Mixer _(k_s,k_c) | |
|----------|----------|--------|--------|----------------------|--------|---------------|--------|-----------|--|---------------|
| | | | | | | | | | (1, 2) | (1, 3) |
| Beauty | Prms(M) | 0.0 | - | 1.18 | 1.18 | 1.31 | 0.79 | 0.81 | 0.81 | 0.81 |
| | FLOPs(M) | 0.0 | - | 14.58 | 7.60 | 16.38 | 10.90 | 11.95 | 11.95 | 11.95 |
| | HR@1 | 0.0077 | 0.0407 | 0.0651 | 0.0792 | 0.0988 | 0.0959 | 0.1068 | 0.1104 | <u>0.1102</u> |
| | HR@10 | 0.0762 | 0.2142 | 0.2676 | 0.2803 | 0.3272 | 0.3217 | 0.3244 | 0.3294 | <u>0.3278</u> |
| | NDCG@10 | 0.0349 | 0.1124 | 0.1479 | 0.1518 | 0.2000 | 0.1950 | 0.2029 | 0.2076 | <u>0.2073</u> |
| Steam | Prms(M) | 0.0 | - | 1.18 | 1.18 | 1.31 | 0.79 | 0.81 | 0.81 | 0.81 |
| | FLOPs(M) | 0.0 | - | 12.46 | 5.48 | 14.26 | 8.77 | 9.82 | 9.83 | 9.83 |
| | HR@1 | 0.0159 | 0.0246 | 0.0832 | 0.0986 | 0.1368 | 0.1138 | 0.1204 | 0.1278 | <u>0.1305</u> |
| | HR@10 | 0.1389 | 0.2169 | 0.3685 | 0.4011 | 0.4560 | 0.4227 | 0.4245 | <u>0.4430</u> | <u>0.4413</u> |
| | NDCG@10 | 0.0665 | 0.1026 | 0.2153 | 0.2315 | 0.2761 | 0.2476 | 0.2525 | <u>0.2635</u> | <u>0.2657</u> |
| ML-1m | Prms(M) | 0.0 | - | 1.18 | 1.18 | 1.31 | 0.87 | 0.89 | 0.89 | 0.89 |
| | FLOPs(M) | 0.0 | - | 47.36 | 19.44 | 60.69 | 35.67 | 36.82 | 36.83 | 36.83 |
| | HR@1 | 0.0141 | 0.0397 | 0.2235 | 0.2631 | 0.3018 | 0.2823 | 0.2864 | <u>0.2908</u> | 0.2885 |
| | HR@10 | 0.1358 | 0.3477 | 0.6374 | 0.6612 | 0.7128 | 0.6958 | 0.6992 | <u>0.7009</u> | 0.7039 |
| | NDCG@10 | 0.0621 | 0.1640 | 0.4151 | 0.4468 | 0.4964 | 0.4781 | 0.4805 | <u>0.4873</u> | 0.4853 |

Table 4: Effects of d_s for the token-mixer in MOI-Mixer_(1,1). The results indicate NDCG@10 for ML-1m.

| Model | 16 | 32 | 64 | 128 | 256 | 512 |
|----------------------|--------|--------|--------|---------------|--------|---------------|
| MOI _(1,1) | 0.4485 | 0.4652 | 0.4737 | <u>0.4805</u> | 0.4791 | 0.4814 |

We also observe that MOI-Mixer_(1,1) works reasonably well with a wide range of token hidden dimensions as described in Table 4. Although ML-1m’s maximum sequence length is set to $s = 200$, utilizing a bottleneck architecture of $d_s = 128$ showed subtle performance difference to $d_s = 512$. Moreover, in the extreme case of encoding the interactions with $d_s = 16$, the performance dropped only by 3.2%.

From these experimental results, we claim that the token-mixing operation of sequential recommendation may not require complex interactions and a simple interaction may be sufficient.

Table 5: Effects of the channel interaction orders on ML-1m.

| Model | k_s | k_c | Params (M) | NDCG@10 |
|-----------|-------|-------|------------|---------------|
| MOI-Mixer | 1 | 1 | 0.89 | 0.4805 |
| | 1 | 2 | 0.89 | <u>0.4873</u> |
| | 1 | 3 | 0.89 | 0.4853 |
| BERT4Rec | - | - | 1.31 | 0.4964 |

Order of channel interaction Table 5 reports the results of MOI-Mixer for different channel interaction orders $k_c \in \{1, 2, 3\}$. We discovered that increasing the order of channel interaction from $k_c = 1$ to $k_c = 2$ boosts the performance by 0.7%. A possible explanation is that MOI-Mixer benefits from the attained fine-grained

channel representations by explicitly expressing the multiplicative channel interaction as in [15]. Interestingly, when we raise the order of channel interaction from $k_c = 2$ to $k_c = 3$, it does not improve the performance of our model while the results are similarly good, with a performance drop of 0.2%.

In summary, we found that the high-order interaction was helpful in the channel-mixing layer but was not a necessary component in the token-mixing layer. Therefore, unless specified, we will use MOI-Mixer_(1,2), which showed superior performance over MOI-Mixer_(1,3), as our default architecture throughout the paper. We provide additional analysis regarding the impact of different combinations of token- and channel-mixing interaction order on the performance of MOI-Mixer in the Appendix A.1.

5.3 Results

Here, we empirically study the performance of our method on various types of experimental settings. We categorize the datasets as small-scale, large-scale, and long-sequence, to evaluate our model. For all evaluations, we omit NDCG@1 as it is identical to HR@1.

Small-scale Table 3 summarizes the results of all models on Beauty, Steam and ML-1m. First, by comparing POP with NCF, we observe that reflecting the user’s personal preferences is beneficial. Second, explicitly modeling the temporal dynamic with recurrent layers (i.e., GRU4Rec⁺, HPMN) outperform the matrix factorization-based method (i.e., NCF). Third, BERT4Rec significantly outperforms the models with the recurrent layers verifying the effectiveness of the self-attention layers in capturing the user’s preference.

Among the MLP-based methods, MOI-Mixer shows the best performance for all datasets. For Beauty, MOI-Mixer attained state-of-the-art performance with 0.76% higher NDCG@10 results, 38.2% fewer parameters and 27% fewer FLOPs compared to the Transformer-based model (i.e., BERT4Rec). Though MOI-Mixer was not the best

performing architecture for Steam and ML-1m, it achieves competitive results compared to the Transformer-based model (i.e., BERT4Rec). More specifically, compared to MLP-Mixer, MOI-Mixer shows 1.1% and 0.68% improvements in NDCG@10 for Steam and ML-1m, respectively, with identical computational cost. It is interesting to note that MOI-Mixer_(1,2) achieved superior performance to MOI-Mixer_(1,3) for Beauty and ML-1m but not for Steam. We conjecture that the Steam dataset requires more complex features than other datasets when expressing the tokens.

In summary, we demonstrate the importance of including high-order channel interactions to obtain the effective representation for the sequential recommendation datasets at a relatively small scale.

Table 6: The number of parameters of each model with a different number of layers and hidden dimensions.

| Name | Dimensions | | Params (M) | | | |
|-------|------------|-------|------------|------|-----------|-----------|
| | L | d_h | BERT4Rec | gMLP | MLP Mixer | MOI Mixer |
| Base | 12 | 512 | - | 19.4 | 20.1 | 20.1 |
| | 8 | 512 | 21.0 | 12.9 | 13.4 | 13.4 |
| Small | 4 | 512 | 10.5 | 6.5 | 6.7 | 6.7 |
| | 4 | 256 | 2.6 | 1.8 | 1.8 | 1.8 |
| Micro | 2 | 256 | 1.3 | 0.9 | 0.9 | 0.9 |

Large-scale Here, we study the scalability of MOI-Mixer compared to BERT4Rec, gMLP, and MLP-Mixer in a larger dataset, i.e., ML-20m. Table 7 reports the number of parameters for each model by changing the number of layers and hidden dimensions where the configurations are adopted from [4].

Table 7: Performance comparison on ML-20m dataset using the largest model configuration.

| Model | Prms (M) | FLOPs (M) | HR@10 | NDCG@10 |
|-----------|----------|-----------|---------------|---------------|
| BERT4Rec | 21.0 | 906.4 | 0.7756 | 0.5647 |
| gMLP | 19.4 | 806.3 | 0.7712 | <u>0.5622</u> |
| MLP-Mixer | 20.1 | 882.1 | 0.7684 | 0.5580 |
| MOI-Mixer | 20.1 | 882.9 | <u>0.7730</u> | 0.5620 |

Table 7 summarizes the performance of the models with their largest configurations. We found that the performance difference was marginal, showing the largest difference of NDCG@10 was only 0.67%. Among the MLP-based architectures, MOI-Mixer shows competitive scalability against gMLP, which is the state-of-the-art MLP-based architecture in natural language processing tasks [22].

Fig. 4 summarizes the performance vs parameter curve for each model. Comparing BERT4Rec with the MLP-based architectures, the performance gap reduces as the model scale increases. Moreover, MOI-Mixer and gMLP were able to surpass MLP-Mixer at all scales. This verifies that an explicit high-order term is consistently beneficial for learning sequential patterns.

In summary, similar to the findings from the small-scale datasets, the explicit high-order feature interactions were also beneficial for the large-scale dataset.

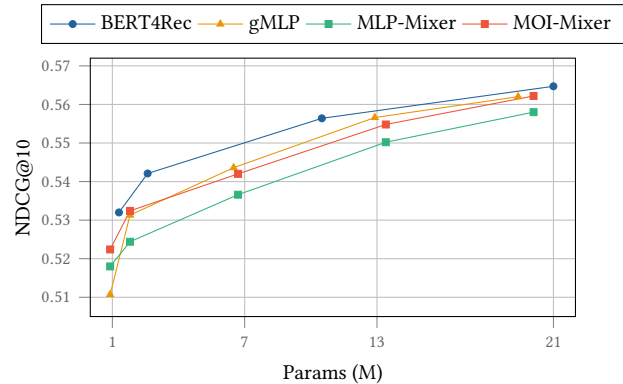


Figure 4: Performance-parameter trade-offs at a different scale, evaluated on ML-20m dataset.

Table 8: Performance of recommendation models on XLong dataset. The maximum sequence length s is set to 1000.

| Model | Prms (M) | VRAM (GB) | FLOPs (M) | NDCG@10 |
|----------------------|----------|-----------|-----------|---------------|
| GRU4Rec ⁺ | 0.14 | 4.37 | 14.75 | 0.1249 |
| HPMN | 0.14 | 3.54 | 6.07 | 0.2657 |
| BERT4Rec | 0.08 | 42.09 | 67.28 | 0.4852 |
| gMLP | 2.05 | 13.14 | 35.40 | 0.4902 |
| MLP-Mixer | 0.30 | 13.32 | 13.04 | <u>0.4914</u> |
| MOI-Mixer | 0.30 | 13.52 | 13.08 | 0.4938 |

Long Sequence Table 8 summarizes the results of GRU4Rec⁺, HPMN, BERT4Rec, gMLP, MLP-Mixer and MOI-Mixer for the XLong dataset. Our goal is to investigate the performance and capacity of each model for modeling lifelong sequences. To fully compare the computational complexity of each model, we set $d_h = 64$, the batch size as 128, and measure all metrics on two RTX 3090 24GB GPUs. Our observations from the results are as follows:

MOI-Mixer achieves the best performance while maintaining identical computation cost of MLP-Mixer, confirming the benefit of high-order interaction for long sequences. MOI-Mixer only required 85.4% fewer parameters and 63.1% fewer FLOPs compared to gMLP, which shows the lowest performance out of all MLP-based models. Moreover, MOI-Mixer required 67.9% fewer VRAM and 80.6% fewer FLOPs than BERT4Rec with 0.86% higher NDCG@10 results.

Fig. 5 illustrates the computation cost and NDCG@10 of the compared models by changing the sequence length s from 100 to 1000. We find that all models yield better recommendation accuracy when given longer sequences, demonstrating the importance of integrating long sequence of interactions. However, in BERT4Rec, the required VRAM and FLOPs grow exponentially with longer sequences due to the attention weight, which is quadratic to a sequence length, and in gMLP, the total number of parameters and FLOPs grow exponentially. Such properties limit the applicability of BERT4Rec and gMLP for real-world tasks requiring modeling

long sequences. In contrast, MLP-Mixer and MOI-Mixer efficiently processes long sequences in linear computational complexity.

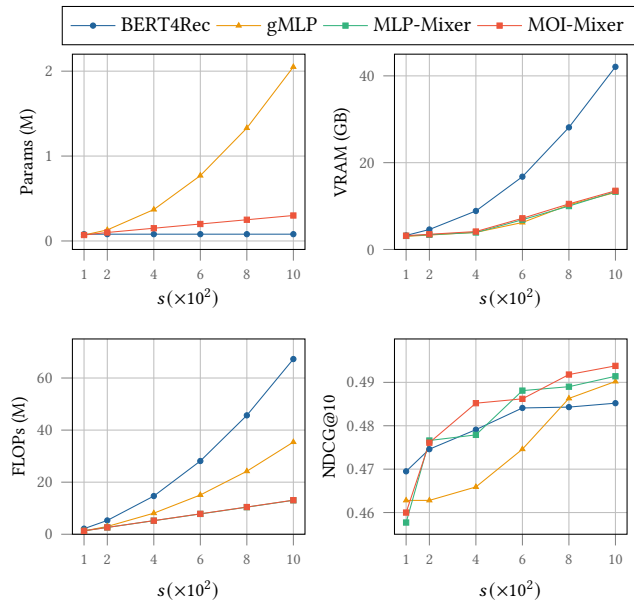


Figure 5: Comparison of different recommendation models in terms of the computational cost and performance. The results are obtained from XLong dataset.

5.4 Ablation studies

Table 9 reports the ablation study of our base model and a summary of our preliminary exploration.

Table 9: Ablation study on the architectural components of MOI-Mixer, evaluated on ML-1m dataset.

| Ablation | Variant | NDCG@10 |
|---------------|-------------------------------------|---------|
| Baseline | MOI-Mixer _(1,2) | 0.4873 |
| Norm-Type | LayerNorm \rightarrow None | 0.4848 |
| | LayerNorm \rightarrow L2-Norm | 0.4767 |
| | LayerNorm \rightarrow Layer-Scale | 0.4862 |
| Norm-Location | Before-Activation | 0.4840 |
| | After-Activation | 0.4859 |
| Token-mixer | MLP \rightarrow Linear | 0.4843 |
| Embedding | (+) Position Embedding | 0.4876 |

Normalization To see how different types of normalization can affects our model performance, we experimented using (i) no normalization, (ii) L2 normalization as in [1] and (iii) Layer Scale [34]. It was interesting to observe that applying L2 normalization degrades the performance more than when applying no normalization at all. Also, while Layer Scale was shown to improve Transformer architectures, MOI-Mixer does not benefit much from it. We also performed

ablation studies to see whether the location of the normalization layer is critical. Through preliminary experiments, we observed that applying the normalization layer right after computing the Hadamard Product was the most effective.

Token-mixer Replacing the MLP layer with a single linear layer for the token-mixing component also gives a good performance, with only a 0.3% decrease in NDCG@10. However, such replacement is not desirable since it creates a quadratic term for the sequence length, restricting the scalability of MOI-Mixer.

Embedding Layer Following the implementation details of Transformer, we also evaluated the performance of MOI-Mixer with additionally applying positional embeddings. The position embedding did not bring gain to MOI-Mixer since the MLP layer is already sensitive to the order of the sequences.

6 CONCLUSION AND DISCUSSION

This paper proposed MOI-Mixer, which aims to leverage high-order interactions for MLP-based models in sequential recommendation systems. We claim that Transformer and existing MLP-based models differ in performance due to the absence of an explicit high-order term. Thus, we introduce a novel MOI layer which is capable of modeling arbitrary multi-order interactions among the given input features. Experimental results on five real-world datasets show that integrating a high-order term in MLP-based models is consistently beneficial. We also show that MOI-Mixer is computationally efficient in processing long-sequence behavior data compared to the state-of-the-art model [29].

Interesting future work includes applying MOI-Mixer to various other fields such as computer vision and natural language processing, where the simple MLP-based models have shown competitive results. We hope that our work opens up the potentials for research on MLP-based models in sequential recommendation tasks.

A APPENDIX: ADDITIONAL EXPERIMENTS

A.1 Analysis on the interaction orders

The following table reports the results of MOI-Mixer by varying the order of the token- and the channel-mixing layers.

Table 10: MOI-Mixer’s performance on ML-1m dataset by varying the combinations of the interaction orders.

| $k_s \setminus k_c$ | 1 | 2 | 3 | 4 |
|---------------------|--------|---------------|--------|---------------|
| 1 | 0.4805 | 0.4873 | 0.4853 | <u>0.4855</u> |
| 2 | 0.4782 | 0.4846 | 0.4835 | 0.4812 |
| 3 | 0.4674 | 0.4743 | 0.4729 | 0.4711 |
| 4 | 0.4653 | 0.4738 | 0.4708 | 0.4695 |

In this table, we observe that (i) increasing interaction order between the tokens consistently degrades the performance regardless of the channel’s interaction order and (ii) the second-order channel interaction performed the best where further increasing the order of channel interactions weakens the performance in MOI-Mixer.

REFERENCES

- [1] Saadullah Amin, Stalin Varanasi, Katherine Ann Dunfield, and Günter Neumann. 2020. LowFER: Low-rank Bilinear Pooling for Link Prediction. In *PMLR*.
- [2] Jimmy Lei Ba, Jamie Ryan Kiros, and Geoffrey E Hinton. 2016. Layer Normalization. (2016).
- [3] Seokju Cho, Sunghwan Hong, Sangryul Jeon, Yunsung Lee, Kwanghoon Sohn, and Seungryong Kim. 2021. Semantic Correspondence with Transformers. *arXiv preprint arXiv:2106.02520* (2021).
- [4] Jacob Devlin, Ming-Wei Chang, Kenton Lee, and Kristina Toutanova. 2018. Bert: Pre-training of deep bidirectional transformers for language understanding. *arXiv preprint arXiv:1810.04805* (2018).
- [5] Tuong Do, Thanh-Toan Do, Huy Tran, Erman Tjiputra, and Quang D Tran. 2019. Compact trilinear interaction for visual question answering. In *Proc. of the IEEE international conference on computer vision (ICCV)*. 392–401.
- [6] Alexey Dosovitskiy, Lucas Beyer, Alexander Kolesnikov, Dirk Weissenborn, Xiaohua Zhai, Thomas Unterthiner, Mostafa Dehghani, Matthias Minderer, Georg Heigold, Sylvain Gelly, et al. 2020. An Image is Worth 16x16 Words: Transformers for Image Recognition at Scale. In *International Conference on Learning Representations*.
- [7] Kaiming He, Xiangyu Zhang, Shaoqing Ren, and Jian Sun. 2016. Deep residual learning for image recognition. In *Proc. of the IEEE conference on computer vision and pattern recognition (CVPR)*.
- [8] Xiangnan He, Lizi Liao, Hanwang Zhang, Liqiang Nie, Xia Hu, and Tat-Seng Chua. 2017. Neural collaborative filtering. In *Proc. the International Conference on World Wide Web (WWW)*. 173–182.
- [9] Dan Hendrycks and Kevin Gimpel. 2020. Gaussian Error Linear Units (GELUs). arXiv:1606.08415 [cs.LG]
- [10] Balázs Hidasi, Alexandros Karatzoglou, Linas Baltrunas, and Domonkos Tikk. 2016. Session-based Recommendations with Recurrent Neural Networks. In *ICLR*.
- [11] Wang-Cheng Hidasi and Julian McAuley. 2018. Session-based recommendations with recurrent neural networks. *Proc. the IEEE International Conference on Data Mining (ICDM)*.
- [12] S. Hochreiter, Y. Bengio, P. Frasconi, and J. Schmidhuber. 2001. Gradient flow in recurrent nets: the difficulty of learning long-term dependencies. In *A Field Guide to Dynamical Recurrent Neural Networks*. IEEE Press.
- [13] Kurt Hornik, Maxwell Stinchcombe, and Halbert White. 1989. Multilayer feed-forward networks are universal approximators. *Neural networks* 2, 5 (1989), 359–366.
- [14] Liang Hu, Jian Cao, Guandong Xu, Jie Wang, Zhiping Gu, and Longbing Cao. 2013. Cross-domain collaborative filtering via bilinear multilevel analysis. In *Proc. the International Joint Conference on Artificial Intelligence (IJCAI)*.
- [15] Tongwen Huang, Zhiqi Zhang, and Junlin Zhang. 2019. FiBiNET: Combining Feature Importance and Bilinear Feature Interaction for Click-through Rate Prediction. In *RecSys*.
- [16] Wang-Cheng Kang and Julian McAuley. 2018. Self-attentive sequential recommendation. In *Proc. the IEEE International Conference on Data Mining (ICDM)*. 197–206.
- [17] Henk AL Kiers. 2000. Towards a standardized notation and terminology in multiway analysis. *Journal of Chemometrics: A Journal of the Chemometrics Society* 14, 3 (2000), 105–122.
- [18] Jin-Hwa Kim, Jaehyun Jun, and Byoung-Tak Zhang. 2018. Bilinear Attention Networks. *NIPS*.
- [19] Jin-Hwa Kim, Kyoung-Woon On, Woosang Lim, Jeonghee Kim, Jung-Woo Ha, and Byoung-Tak Zhang. 2016. Hadamard product for low-rank bilinear pooling. *ICLR* (2016).
- [20] Diederik P Kingma and Jimmy Ba. 2014. Adam: A method for stochastic optimization. *Proc. the International Conference on Learning Representations (ICLR)* (2014).
- [21] Tamara G Kolda and Brett W Bader. 2009. Tensor decompositions and applications. *SIAM Rev.* 51, 3 (2009), 455–500.
- [22] Hanxiao Liu, Zihang Dai, David R So, and Quoc V Le. 2021. Pay Attention to MLPs. *arXiv preprint arXiv:2105.08050* (2021).
- [23] Ilya Loshchilov and Frank Hutter. 2016. Sgdr: Stochastic gradient descent with warm restarts. *arXiv preprint arXiv:1608.03983* (2016).
- [24] Chen Ma, Liheng Ma, Yingxue Zhang, Jianing Sun, Xue Liu, and Mark Coates. 2020. Memory augmented graph neural networks for sequential recommendation. In *Proc. the AAAI Conference on Artificial Intelligence (AAAI)*, Vol. 34. 5045–5052.
- [25] Julian McAuley, Christopher Targett, Qinfeng Shi, and Anton Van Den Hengel. 2015. Image-based recommendations on styles and substitutes. In *Proc. the ACM Conference on Research and Development in Information Retrieval (SIGIR)*. 43–52.
- [26] Kan Ren, Jiarui Qin, Yuchen Fang, Weinan Zhang, Lei Zheng, Weijie Bian, Guorui Zhou, Jian Xu, Yong Yu, Xiaoqiang Zhu, et al. 2019. Lifelong sequential modeling with personalized memorization for user response prediction. In *Proc. the ACM Conference on Research and Development in Information Retrieval (SIGIR)*. 565–574.
- [27] Steffen Rendle, Christoph Freudenthaler, and Lars Schmidt-Thieme. 2010. Factorizing Personalized Markov Chains for Next-Basket Recommendation. In *WWW*.
- [28] Suvash Sedhain, Aditya Krishna Menon, Scott Sanner, and Lexing Xie. 2015. Autorec: Autoencoders meet collaborative filtering. In *Proc. the International Conference on World Wide Web (WWW)*. 111–112.
- [29] Fei Sun, Jun Liu, Jian Wu, Changhua Pei, Xiao Lin, Wenwu Ou, and Peng Jiang. 2019. BERT4Rec: Sequential Recommendation with Bidirectional Encoder Representations from Transformer. In *Proc. the ACM Conference on Information and Knowledge Management (CIKM)*.
- [30] Jiayi Tang and Ke Wang. 2018. Personalized top-n sequential recommendation via convolutional sequence embedding. In *Proc. of the Web Search and Data Mining (WSDM)*. 565–573.
- [31] Yuki Tatsumi and Masato Taki. 2021. RaftMLP: Do MLP-based Models Dream of Winning Over Computer Vision? arXiv:2108.04384 [cs.CV]
- [32] Ilya Tolstikhin, Neil Houlsby, Alexander Kolesnikov, Lucas Beyer, Xiaohua Zhai, Thomas Unterthiner, Jessica Yung, Daniel Keysers, Jakob Uszkoreit, Mario Luccic, et al. 2021. Mlp-mixer: An all-mlp architecture for vision. *arXiv preprint arXiv:2105.01601* (2021).
- [33] Hugo Touvron, Piotr Bojanowski, Mathilde Caron, Matthieu Cord, Alaeldin El-Nouby, Edouard Grave, Gautier Izacard, Armand Joulin, Gabriel Synnaeve, Jakob Verbeek, and Hervé Jégou. 2021. ResMLP: Feedforward networks for image classification with data-efficient training. *arXiv preprint arXiv:2105.03404* (2021).
- [34] Hugo Touvron, Matthieu Cord, Alexandre Sablayrolles, Gabriel Synnaeve, and Hervé Jégou. 2021. Going deeper with Image Transformers. arXiv:2103.17239 [cs.CV]
- [35] Ashish Vaswani, Noam Shazeer, Niki Parmar, Jakob Uszkoreit, Llion Jones, Aidan N Gomez, Łukasz Kaiser, and Illia Polosukhin. 2017. Attention is all you need. In *Advances in neural information processing systems*. 5998–6008.
- [36] Chao-Yuan Wu, Amr Ahmed, Alex Beutel, Alexander J. Smola, and How Jing. 2017. Recurrent Recommender Networks. In *WSDM*.
- [37] Yongji Wu, Lu Yin, Defu Lian, Mingyang Yin, Neil Zhenqiang Gong, Jingren Zhou, and Hongxia Yang. 2021. Rethinking Lifelong Sequential Recommendation with Incremental Multi-Interest Attention. *arXiv preprint arXiv:2105.14060* (2021).
- [38] Tan Yu, Xu Li, Yunfeng Cai, Mingming Sun, and Ping Li. 2021. S²-MLP: Spatial-Shift MLP Architecture for Vision. arXiv:2106.07477 [cs.CV]
- [39] Heliang Zheng, Jianlong Fu, Zheng-Jun Zha, and Jiebo Luo. 2019. Learning Deep Bilinear Transformation for Fine-grained Image Representation.